Bacterial cellulose growth on 3D acrylate-based microstructures fabricated by two-photon polymerization

Journal of Physics: Photonics

OPEN ACCESS

RECEIVED
27 October 2020

REVISED
13 January 2021

ACCEPTED FOR PUBLICATION
26 January 2021

PUBLISHED
17 February 2021

PAPER

Bacterial cellulose growth on 3D acrylate-based microstructures fabricated by two-photon polymerization

Adriano J G Otuka[1], Rafael R Domeneguetti[2], Jonathas Q R Moraes[1], Debora T Balogh[1], Sidney J L Ribeiro[2] and Cleber R Mendonça[1]

[1] São Carlos Institute of Physics, University of São Paulo, São Carlos 13560-970, SP, Brazil
[2] Institute of Chemistry, São Paulo State University (UNESP), Araraquara 14800-060, SP, Brazil

E-mail: otuka@ifsc.usp.br and crmendon@ifsc.usp.br

Keywords: two-photon polymerization, acrylate-based materials, bacterial cellulose growth

Abstract

Miniaturized environments have emerged as an excellent alternative to evaluate and understand biological mechanisms. These systems are able to simulate macroenvironments with high reproducibility, achieving many results in a short time of analysis. However, microenvironments require specific architectures that can be reached using laser micromachining techniques, such as two-photon polymerization (TPP). This technique has many advantages, allowing the production of environments without shape limitation and with special features. In this work, aided by the TPP technique, we produce different arrays of microstructures, fabricated using acrylate-based materials, in order to evaluate the growth and development of the *Komagataeibacter xylinus* bacteria, the micro-organism responsible for producing bacterial cellulose (BC), a natural polymer with several biological applications. BC grown in microenvironments presents similar features to those of biofilm formed in macroenvironments, maintaining their attractive properties. In addition, due to the high optical quality and mechanical resistance of the BC matrices, we use these films as flexible substrates in TPP experiments, obtaining promising results for tissue engineering studies.

1. Introduction

Biomimetic systems with micrometric dimensions can be used in several experiments, achieving fast results and with great accuracy, similar to analyses performed in macroscopic environments. These platforms have emerged as a promising alternative to studying biological mechanisms, aiming, for instance, to understand the movement dynamics of micro-organisms and their growth in controlled environments [1–6]. An interesting micro-organism that can be explored in miniaturized environments is *Komagataeibacter xylinus*, a species of bacteria responsible for synthesizing bacterial cellulose (BC) [7, 8], a natural renewable polymer. BC presents a uniform structure and morphology. It is also free of lignin and polyoses. It is endowed with unique characteristics, such as high purity and crystallinity, remarkable mechanical properties, good chemical stability, and high water-holding capacity. BC is featured as a completely biocompatible polymer that can be produced in almost any shape due to its high moldability during formation. Therefore, this is an interesting biomaterial that is distinctive in many aspects. Its discovery has shown tremendous potential as an effective biopolymer in various fields, such as tissue engineering [9–12]. In particular, several studies have been carried out in order to apply BC in dressings and biocompatible scaffolds, aiming at, for instance, efficient drug delivery systems [13, 14].

Among the different tools available for biomimetic microenvironment fabrication, the two-photon polymerization (TPP) technique [15–17] has been widely used due to its distinct advantages. In this maskless technique, the local polymerization allows the fast production of three-dimensional (3D) complex platforms, without shape limitation, with high resolution, and in few steps, which makes it a competitive tool in comparison with other simpler micromachining techniques. Several materials can be used in TPP experiments. Usually, these matrices are mixed together with an organic compound known as a

photoinitiator, a molecule responsible for generating free radicals for the polymerization procedure after laser radiation. For biological applications, biodegradable scaffolds are often required [18, 19]. However, acrylate-based materials are also well known to be biocompatible and non-toxic to several micro-organisms [20–24]. In addition, some studies require a large quantity of 3D scaffolds for different analyses. Therefore, it is possible to use TPP combined with sophisticated replication methodologies, which allow fabrication of several scaffolds with an exceptional reproducibility [24–27]. Beyond that, this technique makes it possible to fabricate structures with specific features, which are developed exclusively for the desired applications [28–34].

In this work, we investigate BC formation in 3D acrylate-based arrays produced via TPP. We compare BC grown on these photopolymerized structures with the matrices obtained by conventional means (macroscopic experiments). In addition, we investigate the movement dynamic of *Komagataeibacter xylinus* bacteria in micrometric labyrinths, evaluating the BC formed after their development. Due to their attractive properties, we also use BC matrices as flexible substrates in TPP experiments, using their porous network to diffuse a liquid through the fabricated microstructures, an interesting feature for tissue engineering applications.

2. Materials and methods

2.1. Acrylate-based samples for photopolymerization experiments

To perform the photopolymerization experiments, we use two acrylate-based samples. The first sample, here called the hybrid sample, is composed of a mixture of equal proportions of the penta-acrylate monomer, known as *dipentaerythritol pentaacrylate* (SR399—Sartomer), and a silane compound, known as *3-(trimethoxysilyl)propyl methacrylate* (A174—Sigma Aldrich). The acrylate monomer is used to provide mechanical resistance to the final structure while the silane material is responsible for increasing the roughness of the structure, allowing better adhesion for the inoculated bacteria. A few drops of an acylphosphine oxide photoinitiator, *2,4,6-trimethylbenzoylphenyl phosphinate* (Lucirin TPO-L—Irgacure) are also mixed with the previous compounds (3 wt% in the total sample volume). The second sample is prepared using only acrylate monomers. This sample is composed of two three-acrylate monomers, *ethoxylated(6) trimethyl-lolpropanetriacrylate* (SR499—Sartomer) and *tris(2-hydroxyethyl)isocyanuratetryacrylate* (SR368—Sartomer), also employed in equal proportions and mixed with 3 wt% Lucirin TPO-L. Although photoinitiators are often classified as toxic in biological experiments, the Lucirin TPO-L used in the preparation of these samples is known to be a biocompatible compound with several micro-organisms. In addition, the photoinitiator amount used in our experiments is small enough to be almost entirely consumed during the polymerization procedure.

2.2. Experimental setup used in TPP

3D structures were fabricated using a homemade setup which uses a femtosecond laser (mode-locked Ti:sapphire oscillator—KMLabs) as the excitation source, centered at 790 nm, operating at a repetition rate of 86 MHz and delivering pulses of ∼150 fs. The laser beam is focused on the acrylate-based samples (placed between glass substrates separated by a micrometer spacer) using a 10× microscope objective (NA = 0.25, voxel size ∼6 × 1.5 μm). A pair of galvanometric mirrors is controlled by dedicated software, allowing laser scanning through the sample in two dimensions (x–y plane). A translational stage, which also holds the sample during the photopolymerization experiment, is used to achieve the third dimension on the structure. The laser intensity is controlled using a half-wave plate and a polarizer, positioned in front of the galvanometric mirrors. Due to the difference between the refractive index of the solidified resin and the liquid resin [35], the polymerization process can be monitored in real time aided by an independent imaging system composed of a CCD camera, a telescope and a red LED. At the end of the fabrication procedure, the sample is immersed in ethanol heated at 75 °C for 15 min, in order to remove the unpolymerized resin. Finally, before starting the biological experiments, the fabricated microstructures are sterilized using UV irradiation.

2.3. *Komagataeibacter xylinus* activation and BC growth

First, the *Komagataeibacter xylinus* bacteria were activated by transferring the surface of the solid culture plates to a liquid medium [36], where they grew and multiplied. Some BC properties, such as the optical quality and porosity, depend on how the natural polymer is purified (washed) and dried. In figure 1, we can observe three different matrices obtained after distinct washing and drying procedures.

As can be seen in figure 1(a), non-purified BC membranes exhibit a nanofibrous porous network that is highly moldable. Also in figure 1(a), it is possible to observe *Komagataeibacter xylinus* bacteria inside the formed matrix. When water-soaked membranes were put on support and submitted to drying in an

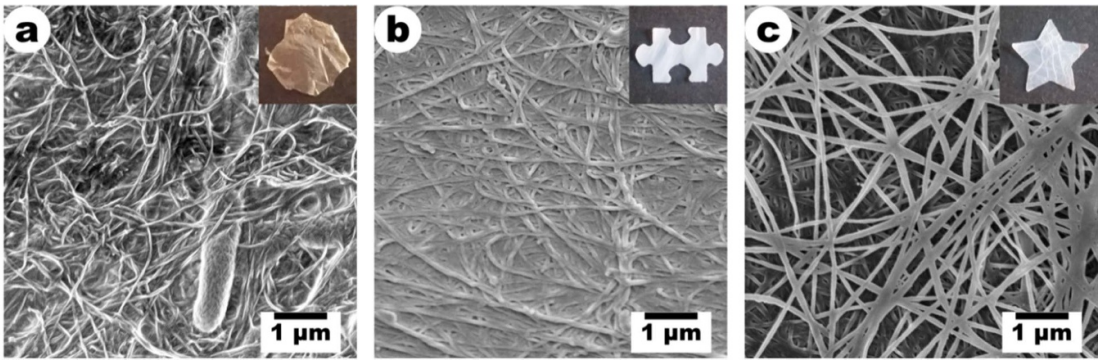

Figure 1. BC matrices obtained after distinct washing and drying procedures. (a) Non-purified BC membrane dried at room temperature. It is possible to see *Komagataeibacter xylinus* bacteria inside the formed matrix. (b) BC membranes washed in water and dried in a forced air circulation oven with temperature control at 28 °C for 12 h. (c) BC membranes washed in ethanol and subjected to supercritical drying in a E3000 critical point dryer (using liquid CO_2 as a solvent).

air-circulation oven with the temperature controlled at 28 °C for 12 h (figure 1(b)), the biofilm porosity decreased and the mechanical stability of the natural polymer was improved. Finally, in figure 1(c), the ethanol-soaked membranes were subjected to supercritical drying in an E3000 critical point dryer (Quorum Technologies) using liquid CO_2 as a solvent. The exchange of ethanol in the pores of the membranes with liquid CO_2 was done by a slow change of solvent over 4 h. Supercritical drying was carried out by heating the system to 45 °C and maintaining the pressure at 1200–1300 psi. The system was maintained under these pressure/temperature conditions for 1 h before venting to obtain the BC membrane aerogel [37]. As a result of this procedure, the BC membranes were highly moldable, with appropriate optical quality and with high porosity degree, an interesting feature for several biomedical applications.

To evaluate the bacteria development in photopolymerized microenvironments, the fabricated structures were placed inside Petri dishes with a water slide at the bottom. With the help of a micropipette, a 5 μl drop of the liquid medium containing the bacteria was placed on the surface of the microstructures. Then, each Petri dish was placed in an incubator with air circulation and temperature control at 28 °C for 24 h. After the above procedure, the plate was frozen and lyophilized.

2.4. Characterization of BC grown on the microstructures

To evaluate and characterize the BC grown on the microstructures, we used conventional optical microscopy, scanning electron microscopy (SEM—Zeiss, SIGMA model) and a Fourier-transform infrared (FT-IR) spectrometer (Bruker, Vertex 70 model using an ATR objective).

3. Results and discussion

This section presents the results as a proof of principles regarding BC formation on the photopolymerized microstructures using hybrid and polymeric matrices. Figure 2 shows typical structures fabricated with hybrid materials (left) and acrylate matrices (right).

Komagataeibacter xylinus bacteria were inoculated into the acrylate-based microenvironments for 24 h, receiving all the necessary conditions for their development (as described in section 2.3).

As can be seen in figure 3, the BC film formed in the array composed of hybrid materials presented good adhesion to the structure surface, including inside the cylinders (as shown in figure 3(b)). It is still possible to observe that the thickness of the formed film was limited by the cylinder size.

FT-IR spectroscopy was performed on these grown films in order to evaluate and compare them with macroscopic BC matrices (grown on the usual platforms or experiments). Figure 4 shows these results.

The ATR-FTIR spectrum of the neat BC matrix (black line) shows characteristic bands of BC. Different bands can be identified in the spectrum, which include hydrogen-bonded hydroxyl groups (O−H stretching around 3100 cm^{-1}–3600 cm^{-1}), CH_2 symmetric (around 2890 cm^{-1}) and asymmetric (around 2850 cm^{-1}) stretching, bending motion of absorbed water H−O−H (1650 cm^{-1} region) and characteristic C–C and C–O–C polysaccharide linkages (multiple bands in the 800–1200 cm^{-1} region) [38, 39]. When a similar analysis was performed on BC films grown on hybrid microstructures, we observed equivalent bands (figure 4, red line), indicating that the BC microfilms have a similar chemical composition to those macroscopic BC films.

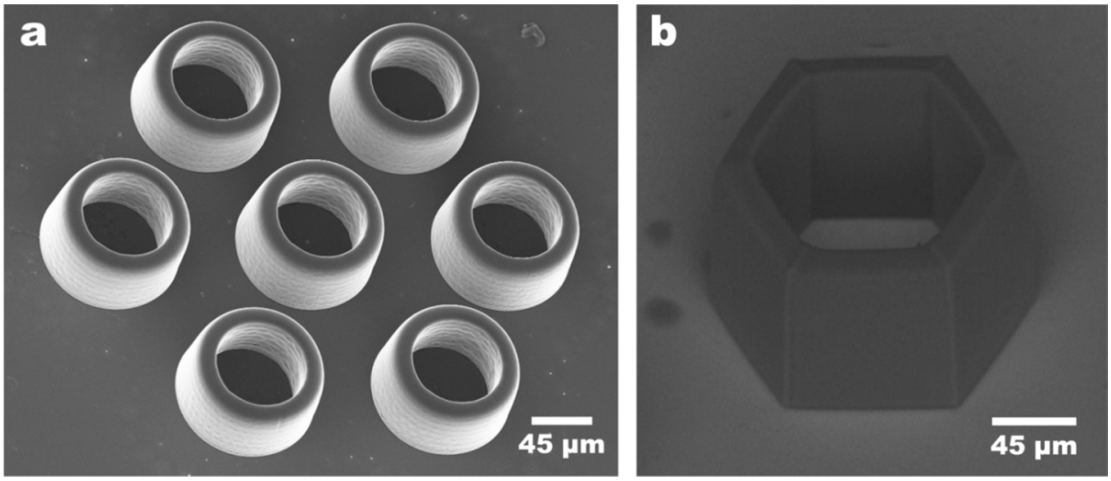

Figure 2. Microstructures fabricated via TPP using acrylate-based materials. (a) Hybrid matrices, which have more roughness on the surface. (b) Polymeric matrices, a typical sample used in TPP experiments.

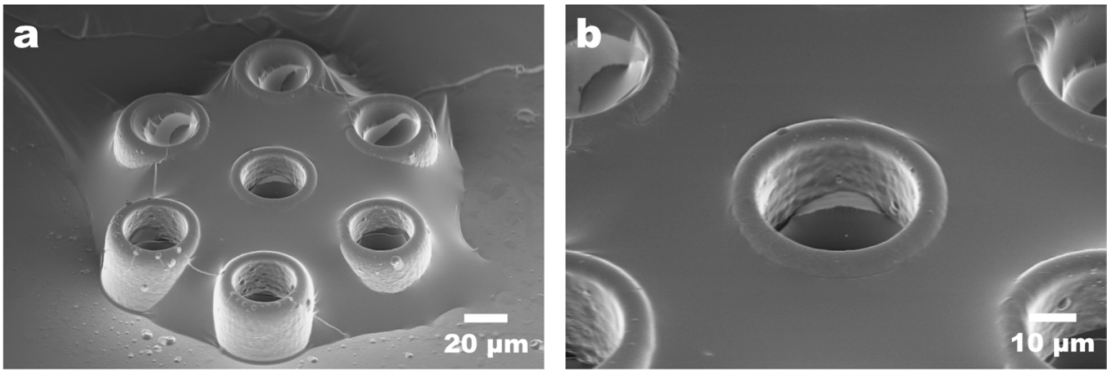

Figure 3. BC grown on the microstructures fabricated with hybrid matrices. (a) It is possible to observe good adhesion of the formed BC film around the microstructures, including (b) inside the cylinders.

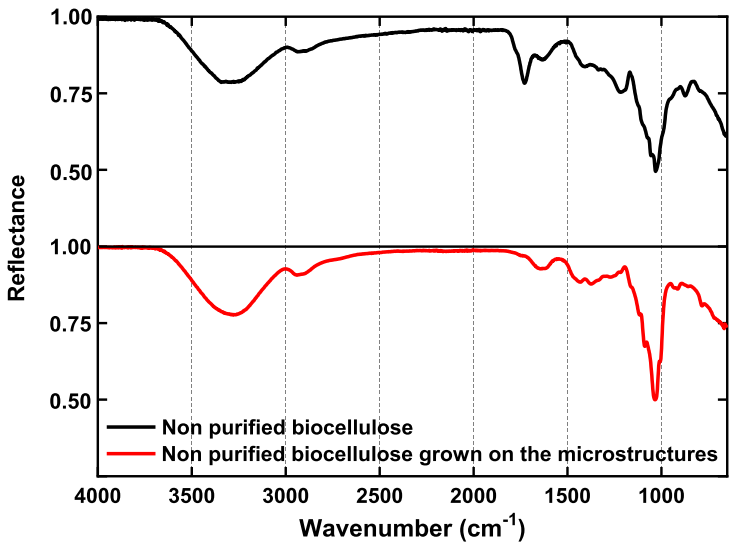

Figure 4. FT-IR spectrum of BC matrices. Black line: macroscopic sample, which was formed according to conventional procedures. Red line: BC formed on the photopolymerized microstructures.

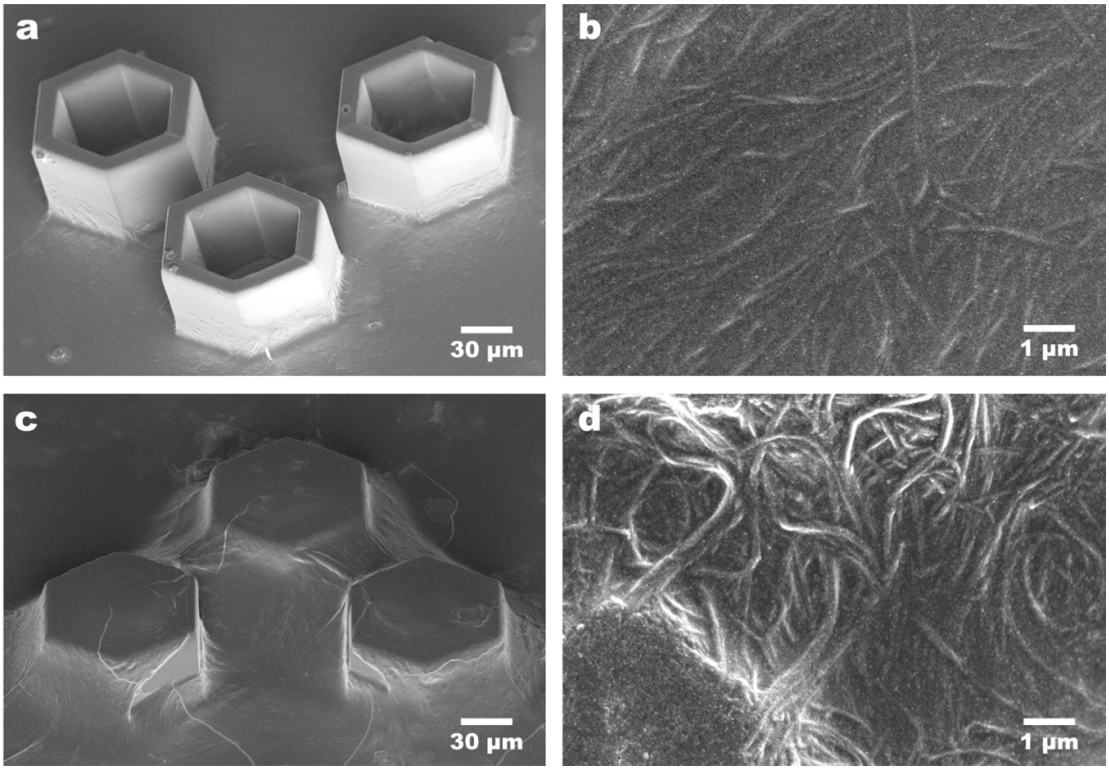

Figure 5. BC grown on polymeric materials. (a) BC film formed after 6 h of bacteria incubation and (b) SEM image of the BC network grown in these structures. (c) BC film formed after 24 h of bacteria incubation and (d) SEM image of the BC network grown in these structures.

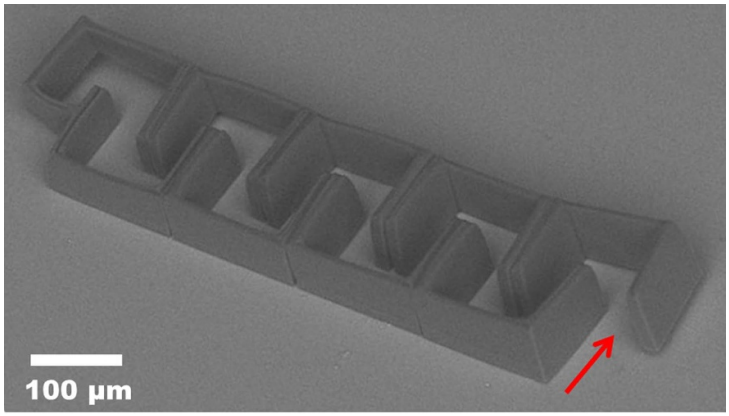

Figure 6. Photopolymerized labyrinth used to evaluate the movement dynamics of *Komagataeibacter xylinus* bacteria and BC film formation. The red arrow indicates the small aperture of the structure.

We also evaluate how the BC is synthesized at different incubation times. Figure 5 shows the results when the bacteria are inoculated into the microenvironments for 6 h (figures 5(a) and (b)) and 24 h (figures 5(c) and (d)).

As shown in figure 5(a), even after a short time of incubation, it is already possible to identify a network of nanofibers around the structures (on the bottom). After 24 h of incubation, it is possible to observe a thin film formed on the microstructures, covering the microenvironment. This result is very interesting because it can enable the removal of BC grown in these structures, allowing their application in other experiments.

To investigate the mobility mechanisms of the *Komagataeibacter xylinus* bacteria, we fabricate micrometric labyrinths. In these structures, there is only a small aperture, which we use to inoculate the bacteria. To facilitate our analyses, the labyrinths do not have a ceiling. Figure 6 shows an SEM image of the fabricated labyrinth, and the red arrow indicates the structure aperture.

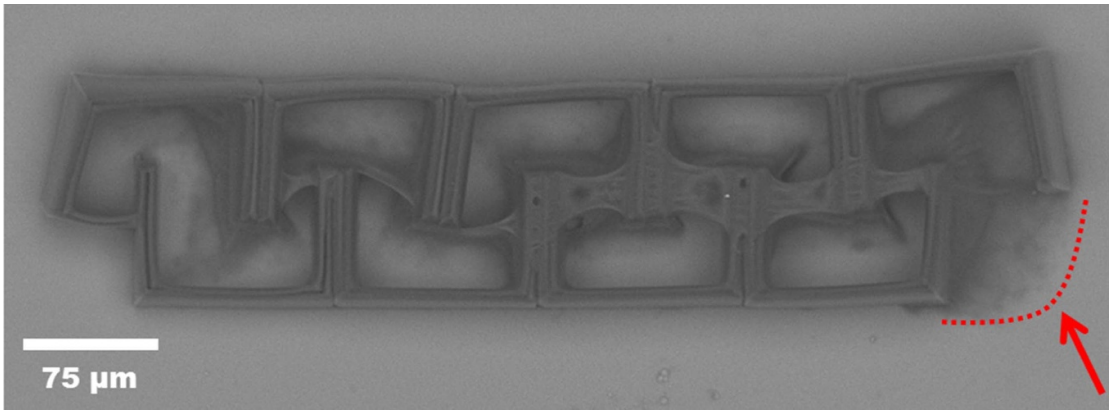

Figure 7. BC grown in the labyrinth after 24 h of bacteria incubation. The bacteria are inoculated around the region indicated by the red dots. It is possible to observe that the BC films grow preferentially over short distances, using the labyrinth walls to support adhesion.

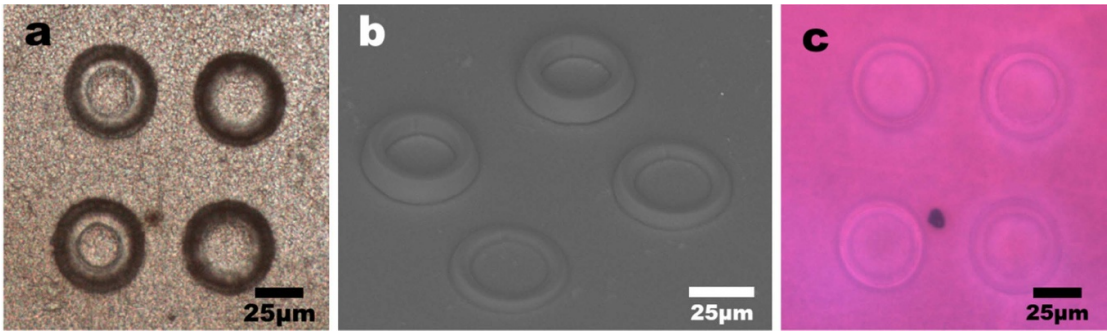

Figure 8. BC used as flexible substrate in TPP experiments. (a) Optical microscopy image of microstructures fabricated on this substrate. (b) SEM image of these structures. (c) Optical microscopy image of microstructures on the flexible substrate, which were immersed in rhodamine B solution for 5 min, and washed three times in ethanol. It is possible to observe liquid diffusion through the BC and fabricated microstructures even after the washing procedure.

Again, the bacteria are inoculated in the environment for 24 h and, posteriorly, we evaluate the BC growth on the structures. The results are presented in figure 7.

Bacteria were dispensed only close to the labyrinth aperture. In this experiment, we observed that the biofilm did not grow throughout the entire labyrinth, but preferentially over short distances ($\sim$30–40 μm), using the structure walls to support the adhesion.

As previously mentioned, BC is a natural highly moldable polymer, which can be applied as a flexible substrate in several devices. In addition, the high porosity of the BC membranes is an attractive feature for different applications aimed at the diffusion of liquid media of interest, such as organic dyes or medicines. Here, we also use BC as a substrate for TPP experiments. Figure 8 summarizes some of the results when we fabricated 3D structures using BC as a support material.

To fabricate these structures we used BC matrices as a support material, as presented in figure 1(c), which have a high pore density. During the TPP experiment, the BC film maintained its properties and structural integrity, an important feature for this application. Figures 8(a) and (b) show, respectively, an optical microscopy image and an SEM image of the fabricated structures. To demonstrate a potential application of these structures fabricated on the flexible substrate, we soaked the sample in a solution of rhodamine B dissolved in ethanol (10^{-4} M) for 5 min and evaluated the liquid diffusion. After this step, we washed the sample (microstructures and BC substrate) three times in ethanol. As can be seen in figure 8(c), it is possible to observe that the liquid spreads in all directions, including inside the photopolymerized structures. Thus, the results obtained in this experiment can open new possibilities for the use of BC as a flexible substrate, allowing future applications in drug delivery systems and in other tissue engineering fields.

4. Conclusion and final remarks

In this work, we presented 3D acrylate-based structures fabricated via TPP, which were used to evaluate the development of *Komagataeibacter xylinus* bacteria, a micro-organism responsible for BC production. BC formation occurred both in hybrid and polymeric matrices, and their original features were kept, as demonstrated by SEM images and FT-IR spectroscopy. However, we observed better adhesion of these bacteria in the hybrid matrices.

When the bacteria were inoculated in labyrinths, differently from what was expected, BC formation did not occur throughout the structure. We observed the BC growth preferentially over short distances, using the structure walls to support film adhesion.

Using BC as a flexible substrate in TPP experiments, we obtained interesting results. The natural polymer did not change by laser irradiation, maintaining its original features until the end of the photopolymerization procedure. There was a good adhesion of the structures with the natural substrate, even after washing the sample in heated ethanol. Finally, when the structures fabricated on BC substrates were immersed in rhodamine B solution, we were able to verify the liquid diffusion through the structures. This result demonstrated a potential application of these flexible substrates for liquid diffusion mechanisms in miniaturized environments, opening, for instance, a new approach for drug delivery systems, which require fast, controlled and directed diffusion of medicines.

Acknowledgments

The authors thank Sartomer and Arkema Brazil for donating the acrylate monomers used in this work. We also thank André L S Romero, Bruno B M Torres and Molíria V dos Santos for their technical assistance during the experiments.

Funding

This work was supported by Fundação de Amparo à Pesquisa do Estado de São Paulo (FAPESP—Grant Nos. 2018/11283-7, 2016/20094-8), Coordenação de Aperfeiçoamento de Pessoal de Nível Superior (CAPES) and Conselho Nacional de Desenvolvimento Científico e Tecnológico (CNPq).

Conflict of interest

The authors declare no conflicts of interest.

ORCID iDs

Adriano J G Otuka https://orcid.org/0000-0002-9496-7225
Rafael R Domeneguetti https://orcid.org/0000-0003-2067-2229

References

[1] Sun F, Casse D, van Kan J A, Ge R W and Watt F 2004 Geometric control of fibroblast growth on proton beam-micromachined scaffolds *Tissue Eng.* **10** 267–72
[2] Tayalia P, Mendonca C R, Baldacchini T, Mooney D J and Mazur E 2008 3D cell-migration studies using two-photon engineered polymer scaffolds *Adv. Mater.* **20** 4494–8
[3] Melissinaki V, Gill A A, Ortega I, Vamvakaki M, Ranella A, Haycock J W, Fotakis C, Farsari M and Claeyssens F 2011 Direct laser writing of 3D scaffolds for neural tissue engineering applications *Biofabrication* **3** 045005
[4] Ovsianikov A, Mironov V, Stampfl J and Liska R 2012 Engineering 3D cell-culture matrices: multiphoton processing technologies for biological and tissue engineering applications *Expert Rev. Med. Devices* **9** 613–33
[5] Connell J L, Ritschdorff E T, Whiteley M and Shear J B 2013 3D printing of microscopic bacterial communities *Proc. Natl Acad. Sci. USA* **110** 18380–5
[6] Accardo A, Blatche M C, Courson R, Loubinoux I, Thibault C, Malaquin L and Vieu C 2017 Multiphoton direct laser writing and 3D imaging of polymeric freestanding architectures for cell colonization *Small* **13** 1700621
[7] Oliveira-Alcantara A V, Abreu A A S, Goncalves C, Fucinos P, Cerqueira M A, Gama F M P, Pastrana L M, Rodrigues S and Azeredo H M C 2020 Bacterial cellulose/cashew gum films as probiotic carriers *Lwt-Food Sci. Technol.* **130** 109699
[8] Santoso S P, Chou C C, Lin S P, Soetaredjo F E, Ismadji S, Hsieh C W and Cheng K C 2020 Enhanced production of bacterial cellulose by *Komactobacter intermedius* using statistical modeling *Cellulose* **27** 2497–509
[9] Barud H G D, da Silva R R, Barud H D, Tercjak A, Gutierrez J, Lustri W R, de Oliveira O B and Ribeiro S J L 2016 A multipurpose natural and renewable polymer in medical applications: bacterial cellulose *Carbohydr. Polym.* **153** 406–20
[10] Ullah H, Santos H A and Khan T 2016 Applications of bacterial cellulose in food, cosmetics and drug delivery *Cellulose* **23** 2291–314
[11] Picheth G F, Pirich C L, Sierakowski M R, Woehl M A, Sakakibara C N, de Souza C F, Martin A A, da Silva R and de Freitas R A 2017 Bacterial cellulose in biomedical applications: a review *Int. J. Biol. Macromol.* **104** 97–106

[12] Moniri M, Moghaddam A B, Azizi S, Rahim R A, Bin Ariff A, Saad W Z, Navaderi M and Mohamad R 2017 Production and status of bacterial cellulose in biomedical engineering *Nanomaterials* **7** 257
[13] Almeida I F, Pereira T, Silva N H C S, Gomes F P, Silvestre A J D, Freire C S R, Sousa Lobo J M and Costa P C 2014 Bacterial cellulose membranes as drug delivery systems: an *in vivo* skin compatibility study *Eur. J. Pharm. Biopharm.* **86** 332–6
[14] Abeer M, Mohd Amin M C I and Martin C 2014 A review of bacterial cellulose-based drug delivery systems: their biochemistry, current approaches and future prospects *J. Pharm. Pharmacol.* **66** 1047–61
[15] Farsari M and Chichkov B N 2009 Two-photon fabrication *Nat. Photon.* **3** 450–2
[16] Li L and Fourkas J T 2007 Multiphoton polymerization *Mater. Today* **10** 30–7
[17] Fourkas J T and Maruo S 2008 Recent progress in multiphoton microfabrication *Laser Photonics Rev.* **2** 100–11
[18] Claeyssens F *et al* 2009 Three-dimensional biodegradable structures fabricated by two-photon polymerization *Langmuir* **25** 3219–23
[19] Malinauskas M *et al* 2014 3D microporous scaffolds manufactured via combination of fused filament fabrication and direct laser writing ablation *Micromachines* **5** 839–58
[20] Driscoll M K, Sun X, Guven C, Fourkas J T and Losert W 2014 Cellular contact guidance through dynamic sensing of nanotopography *ACS Nano* **8** 3546–55
[21] Otuka A J G, Correa D S, Fontana C R and Mendonca C R 2014 Direct laser writing by two-photon polymerization as a tool for developing microenvironments for evaluation of bacterial growth *Mater. Sci. Eng.* C **35** 185–9
[22] Avila O I, Otuka A J G, Tribuzi V, Freitas L M, Serafim R B, Moraes M H, Espreafico E M, Valente V, Fontana C R and Mendonca C R 2014 Fabrication of microenvironments with different geometrical features for cell growth studies *J. Laser Micro Nanoeng.* **9** 248–51
[23] Sun X, Driscoll M K, Guven C, Das S, Parent C A, Fourkas J T and Losert W 2015 Asymmetric nanotopography biases cytoskeletal dynamics and promotes unidirectional cell guidance *Proc. Natl Acad. Sci. USA* **112** 12557–62
[24] Sun X Y, Hourwitz M J, Baker E M, Schmidt B U S, Losert W and Fourkas J T 2018 Replication of biocompatible, nanotopographic surfaces *Sci. Rep.* **8** 12557–62
[25] Koroleva A, Gittard S, Schlie S, Deiwick A, Jockenhoevel S and Chichkov B 2012 Fabrication of fibrin scaffolds with controlled microscale architecture by a two-photon polymerization–micromolding technique *Biofabrication* **4** 015001
[26] Boehm R D, Chen B, Gittard S D, Chichkov B N, Monteiro-Riviere N A, Nasir A and Narayan R J 2014 Two-photon polymerization/micromolding of microscale barbs for medical applications *J. Adhes. Sci. Technol.* **28** 387–98
[27] Koroleva A, Gill A A, Ortega I, Haycock J W, Schlie S, Gittard S D, Chichkov B N and Claeyssens F 2012 Two-photon polymerization-generated and micromolding-replicated 3D scaffolds for peripheral neural tissue engineering applications *Biofabrication* **4** 025005
[28] Ovsianikov A, Ostendorf A and Chichkov B N 2007 Three-dimensional photofabrication with femtosecond lasers for applications in photonics and biomedicine *Appl. Surf. Sci.* **253** 6599–602
[29] Farsari M, Ovsianikov A, Vamvakaki M, Sakellari I, Gray D, Chichkov B N and Fotakis C 2008 Fabrication of three-dimensional photonic crystal structures containing an active nonlinear optical chromophore *Appl. Phys.* A **93** 11–5
[30] Terzaki K, Vasilantonakis N, Gaidukeviciute A, Reinhardt C, Fotakis C, Vamvakaki M and Farsari M 2011 3D conducting nanostructures fabricated using direct laser writing *Opt. Mater. Express* **1** 586–97
[31] Ovsianikov A, Dado-Rosenfeld D, Nuernberger S, Levenberg S, Redl H, Liska R and Stampfl J 2012 Laser fabrication of multi-scale elastic 3D scaffolds *J. Tissue Eng. Regen. Med.* **6** 366
[32] Galanopoulos S, Chatzidai N, Melissinaki V, Selimis A, Schizas C, Farsari M and Karalekas D 2014 Design, fabrication and computational characterization of a 3D micro-valve built by multi-photon polymerization *Micromachines* **5** 505–14
[33] Chatzinikolaidou M, Rekstyte S, Danilevicius P, Pontikoglou C, Papadaki H, Farsari M and Vamvakaki M 2015 Adhesion and growth of human bone marrow mesenchymal stem cells on precise-geometry 3D organic-inorganic composite scaffolds for bone repair *Mater. Sci. Eng.* C **48** 301–9
[34] Tomazio N B, Otuka A J G, Almeida G F B, Rosello-Mecho X, Andres M V and Mendonca C R 2017 Femtosecond laser fabrication of high-Q whispering gallery mode microresonators via two-photon polymerization *J. Polym. Sci.* B **55** 569–74
[35] Baldacchini T, LaFratta C N, Farrer R A, Teich M C, Saleh B E A, Naughton M J and Fourkas J T 2004 Acrylic-based resin with favorable properties for three-dimensional two-photon polymerization *J. Appl. Phys.* **95** 6072–6
[36] Hestrin S and Schramm M 1954 Synthesis of cellulose by *Acetobacter xylinum*. 2. Preparation of freeze-dried cells capable of polymerizing glucose to cellulose *Biochem. J.* **58** 345–52
[37] Ferreira-Neto E P, Ullah S, da Silva T C A, Domeneguetti R R, Perissinotto A P, de Vicente F S, Rodrigues U P and Ribeiro S J L 2020 Bacterial nanocellulose/MoS_2 hybrid aerogels as bifunctional adsorbent/photocatalyst membranes for in-flow water decontamination *ACS Appl. Mater. Interfaces* **12** 41627–43
[38] Oh S Y, Yoo D I, Shin Y, Kim H C, Kim H Y, Chung Y S, Park W H and Youk J H 2005 Crystalline structure analysis of cellulose treated with sodium hydroxide and carbon dioxide by means of X-ray diffraction and FTIR spectroscopy *Carbohydr. Res.* **340** 2376–91
[39] Barud H S, Assuncao R M N, Martines M A U, Dexpert-Ghys J, Marques R F C, Messaddeq Y and Ribeiro S J L 2008 Bacterial cellulose–silica organic–inorganic hybrids *J. Sol-Gel Sci. Technol.* **46** 363–7